

# On the Application of a Vortex Lattice Method to Lifting Bodies Close to a Free Surface

Raffaele SOLARI<sup>a</sup>, Patrizia BAGNERINI<sup>b</sup>, and Giuliano VERNENGO<sup>a,1</sup>

<sup>a</sup>*Department of Electrical, Electronic and Telecommunications Engineering and Naval Architecture (DITEN), University of Genoa, Via Montallegro 1, 16145, GE, Italy*

<sup>b</sup>*Department of Mechanical, Energy, Management and Transportation Engineering (DIME), University of Genoa, Via All'Opera Pia, 15, 16145, GE, Italy*

**Abstract.** The interaction of the free surface with either lifting and non lifting, submerged, bodies moving beneath it is of primary interest in naval architecture. Indeed, there are many examples of possible applications such as rudders, stabilizer fins, hydrofoils among the others. The hydrodynamic problem of a submerged lifting body moving close to a free surface presents several complexities that need to be properly addressed in order to achieve a reliable solution. The problem is studied in the framework of a potential flow theory and solved by using an ad-hoc developed Vortex Lattice Method (VLM). The developed method is described and validated by comparison against available data on a flat plate. The analysis then focuses on the convergence properties of the method, especially with respect to the panel dimensions used for the free surface discretization, and on a sensitivity with respect to some peculiar operating parameters such as the depth of the body with respect to the free surface and the angle of attack with respect to the incoming flow.

**Keywords.** Vortex Lattice Method (VLM), Boundary Element Method (BEM), Partial Differential Equations (PDE), Hydrodynamics, Lifting Bodies

## 1. Introduction

The performance prediction of lifting bodies moving beneath a free surface is a classic problem in hydrodynamics that has been investigated by means of many different numerical techniques, being either potential-flow based methods (1; 2; 3) or based on viscous approaches such as e.g. Reynolds averaged Navier Stokes ones (4; 5). This is a relevant problem also from a purely engineering perspective. This is mainly related to the application to high-speed craft that exploit foil-borne condition, achieving very high reductions of the resistance if compared to conventional operating mode, with a relatively large portion of the hull that is wet (6; 7).

In the proposed study, the continuous form of the BVP representing the specific hydrodynamic problem is solved in the framework of a particular Boundary Ele-

---

<sup>1</sup>Corresponding Author: giuliano.vernengo@unige.it.

ment Method (BEM) that is the Vortex Lattice Method (VLM). This particular numerical method has originally been developed in the field of aerodynamics (8; 9) but it has been successfully applied e.g. for propeller design and analysis (10), hydrofoils analysis (11), planing hull analysis (12; 13; 14; 15).

The analysis focuses on the mathematical and numerical treatment of the free surface boundary conditions and on the sensitivity of the solution with respect to some model parameters and operating conditions.

## 2. Boundary Value Problem for Lifting Bodies with a Free Surface

The hydrodynamic problem of a lifting body travelling close to a free surface is formulated in the framework of a potential flow theory. Being  $\rho$ ,  $\nu$  and  $\xi$  the fluid density, kinematic viscosity and the vorticity, respectively, the fluid is assumed to be inviscid,  $\nu = 0$ , irrotational,  $\xi = 0$ , and incompressible,  $\partial\rho/\partial t = 0$ . According to these hypotheses, the velocity vector  $\mathbf{v}$  can be related to a velocity potential function  $\Phi(x, y, z)$ , i.e. a scalar function defined so that  $\nabla\Phi(x, y, z) = \mathbf{v}$ . Accepting the linearity of the potential flow function, it is found as superimposition of a free stream potential  $\phi_\infty = x \cdot U$  and a potential  $\phi(x, y, z) = [\partial v_x/\partial x, \partial v_y/\partial y, \partial v_z/\partial z]$  due to the disturbance to the flow caused by the body. Then,  $\Phi(x, y, z) = x \cdot U + \phi(x, y, z)$ . A simply connected domain,  $D$ , as the one showed in Figure 1, is considered. It is made of a boundary surface for the lifting body,  $S_b$ , a surface for the wake detached by the trailing edge,  $S_w$ , a free surface,  $S_{fs}$ , and a surface at infinite distance from the body,  $S_\infty$ . Each of these boundary surfaces is used to impose a specific Boundary Condition (BC) then resulting in a particular Boundary Value Problem (BVP). Since the domain with the immersed body is, in principle, non-simply connected the wake is needed to retrieve this property.

The method has been developed for a deep water condition, that is the sea bottom surface  $S_\infty$  is far enough not to affect the solution. This intrinsically fulfills the radiation condition that imposes the decay of the potential function far from the body, without needing any additional condition to the seabed. The BC for the body is the classic non-penetration condition imposed on the derivative of the potential, assuming the form of a Neumann-type condition. So the normal flow velocity at the body surface  $S_b$  must be null. The wake of the lifting body is needed to close the problem by imposing a Kutta type condition.

The remaining BCs are enforced on the free surface. This is a continuous interface whose shape is unknown, then part of the solution, that must fulfill both a kinematic (KBD) and a dynamic (DBC) boundary condition. The first imposes that the free surface

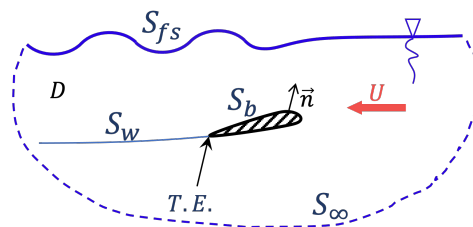


Figure 1. Fluid domain considered for the formulation of the BVP problem.

interface, described in explicit form by  $F = z - \eta(x, y)$ , is always made of the same particles, that is  $\dot{F} = 0$ . The latter belongs to the Bernoulli's theorem and is needed to impose the pressure at this interface equal to the atmospheric one,  $p_{fs} = p_{atm}$ .

The potential flow function can be derived in terms of singular elements such as sources,  $\sigma$ , and doublets (or vortexes),  $\mu$ , by using the Green identity of Eqs. (1). Such a potential function satisfies the Laplace equation  $\nabla^2 \Phi = 0$  in the fluid domain  $D$ .

$$\Phi(x, y, z) = -\frac{1}{4\pi} \int_S \left( \sigma \cdot \frac{1}{r} - \mu \frac{\partial}{\partial n} \frac{1}{r} \right) dS + \phi_\infty \quad (1)$$

The fully non-linear BVP for the lifting body close to a free surface then reads as in the following Eqs. (2). In particular, for a submerged body, there are two sources of non-linearities in the set of PDEs of Eqs. (2), namely the second order terms in the DBC related to the perturbation velocity square and the presence of the unknown terms  $\eta$  and  $\nabla \eta$  in the KBC and in the DBC, respectively.

$$\begin{cases} \nabla^2 \Phi = 0, & \text{in } D \\ \nabla \Phi \cdot \mathbf{n} = 0, & \text{at } S_B \\ \frac{\partial \Phi}{\partial z} - \nabla \Phi \cdot \nabla \eta = 0, & \text{on } z = \eta(x, y) \\ \frac{1}{2} (\nabla \Phi)^2 - \frac{1}{2} U^2 + g\eta = 0, & \text{on } z = \eta(x, y) \\ \lim_{\mathbf{r} \rightarrow \infty} \nabla \Phi = 0, & \text{at } S_\infty \end{cases} \quad (2)$$

### 2.1. Linearization of the BVP

The non-linear characteristic of the system of PDEs previously derived poses both theoretical and computational issues. In principle there can be at least two possible ways to approach it. A first approach would be to use of system of algebraic equations made of the non-penetration BC on the body surface and the KBC at the unknown free surface. Once the unknown singularities strengths have been computed by solving the system, the values of the free surface elevations at each point in the interface should be computed according to the DBC. However, even if it seems to be a possible approach to simplify the solution, it is worth noticing that by the KBC the gradient of the function for the wave elevation is included into the equation. The specific value of the free surface elevation at each point would then be computed according to the DBC. This latter solution is not unique since it is based on the gradient of the function  $\nabla \eta$ . So this process might strongly be affected by the initial solution obtained in terms of derivatives of the free surface shape.

Another option would be to try to solve the system of equations made of the non-penetration BC on the body coupled with the DBC at the free surface. Once the strengths of the singularities have been found the KBC needs to be solved, being careful to properly treat the terms of  $\nabla \eta$  by choosing a suitable numerical derivation scheme.

In the proposed approach the BC on the free surface have been linearized (16; 17; 11). In particular, it is assumed to enforce both the DBC and the KBC at the mean,

June 2022

undisturbed, water level, that is  $z = 0$ . This results in Eqs. 3, that is a single BC which combines the two mentioned ones, then eliminating the unknown  $\eta$ :

$$\frac{1}{2} \nabla \Phi \cdot \nabla (\nabla \Phi)^2 + g \frac{\partial \Phi}{\partial z} = 0, \quad \text{at } z = 0 \quad (3)$$

This equation is then linearized with respect to the higher order terms,  $O(\varepsilon) > 1$ , obtaining the following Eqs. (4):

$$U^2 \frac{\partial^2 \phi}{\partial x^2} + x \frac{\partial \phi}{\partial z} = 0, \quad \text{at } z = 0 \quad (4)$$

The free surface elevation is then computed according to the DBC, as  $\eta = -1/2\pi (\nabla \Phi^2 - U^2)$  or, in its linear form,  $\eta = -U/g \cdot \partial \phi / \partial x$ . According to all the assumptions made, the resulting BVP is then formulated as follows:

$$\begin{cases} \frac{\partial^2 \phi}{\partial x^2} + \frac{\partial^2 \phi}{\partial y^2} + \frac{\partial^2 \phi}{\partial z^2} = 0, & \text{in } D \\ \frac{\partial \phi}{\partial n} + U \cdot n_x = 0, & \text{at } S_B \\ U^2 \frac{\partial^2 \phi}{\partial x^2} + x \frac{\partial \phi}{\partial z} = 0, & \text{at } z = 0 \end{cases} \quad (5)$$

## 2.2. Numerical Treatment of the Free Surface BC

A particular treatment of the free surface BC is needed to adequately propagate the stationary waves generated by the presence of the body. According to the definition of the perturbation potentials, Eqs.4 can be written in terms of induced velocities then reducing the order of the derivative:

$$\frac{\partial}{\partial x} \left( \frac{\partial \phi}{\partial x} \right) + \frac{g}{U^2} \frac{\partial \phi}{\partial z} = \frac{\partial}{\partial x} (u_{ind}) + \frac{g}{U^2} w_{ind} = 0, \quad \text{at } z = 0 \quad (6)$$

Considering the linearized DBC that can be consistently used to compute the posterior free surface elevation, if the collocation points are located at  $z=0$ , that is where the free surface BCs are enforced,  $\partial \phi / \partial x \rightarrow 0$  for  $dh/c \rightarrow 0$ , being  $dh$  and  $c$  the vertical distance between the collocation point and the singularity and the body length (i.e. the chord of a profile), respectively. Even shifting the collocation points by e.g.  $dh/c = 0.15$  a local wave perturbation is obtained that is then numerically damped, as shown in the top left corner of Figure 2. Considering a four points, backward scheme, as suggested by Dawson (16), and a fictitious displacement of the collocation points  $dh/c = 0.15$ , a fully developed wave pattern can be obtained, as shown in the bottom left corner and in the perspective view of Figure 2. The derivative of the potential function at the  $i$ -th panel of the free surface is then computed according to Eqs. (7), based on the values of the induced velocity  $u$  and some particular geometry-related coefficients  $C_j$  at the  $i$ -n panels, with  $n=1,2,3$ .

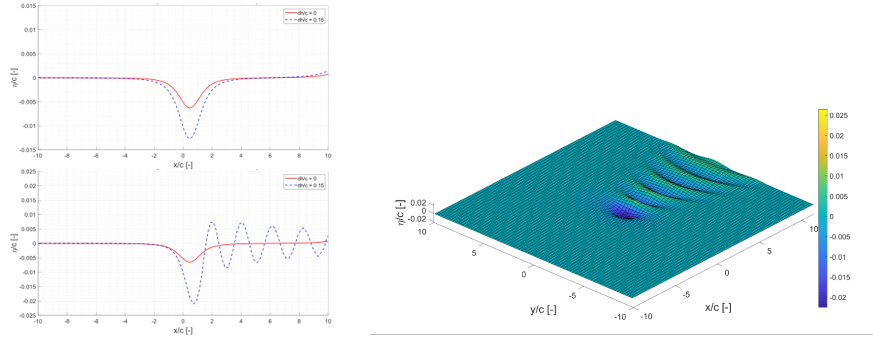


**Figure 2.** Results of the free surface elevation for different derivation schemes. Wave profiles at the symmetry plane with  $dh/c=0.0$  (solid red line) and  $dh/c=0.15$  (dashed blue line) for a two point backward (top left) and four point backward (bottom left) scheme. Right: the 3D wave pattern obtained by using a four point backward finite differences scheme.

$$\left(\frac{\partial\phi}{\partial x}\right)_i = \sum_{j=0}^3 C_j \cdot u_{i-j} \quad (7)$$

### 2.3. Numerical Method for the Solution of the BVP

The continuous for the of the linearized BVP represented in Eqs. (5) is solved by using the Vortex Lattice Method (VLM). According to this approach, both the body (mean camber line) and the free surface are represented by using a structured grid of quadrilateral elements. Each element represents a so called vortex ring. So, a vortex filament of strength  $\Gamma_k$  is associated to each of the  $k$ -th side of the element. The BCs described are fulfilled at the center of each vortex ring, called a collocation point. Since the velocity induced by a vortex filament,  $\mathbf{v}_i$ , can be easily computed according to the Biot-Savart law described in Eqs. (8), the problem is then formulated in terms of induced velocities rather than in terms of velocity potentials. The computation of the velocity induced by a vortex ring is then straightforward as vector summation of the four contributions  $\mathbf{v}_{VR} = \sum_{i=1}^4 \mathbf{v}_i$ . As an example, Figure 3 displays the vertical induced velocity by a unit strength vortex ring at a collocation point that moves along a longitudinal line (dashed red line). It is worth noticing that, with respect to the Green identity in Eqs. (1), a distributino of constant strength vortexes is equivalent to that of uniform doublets (18).

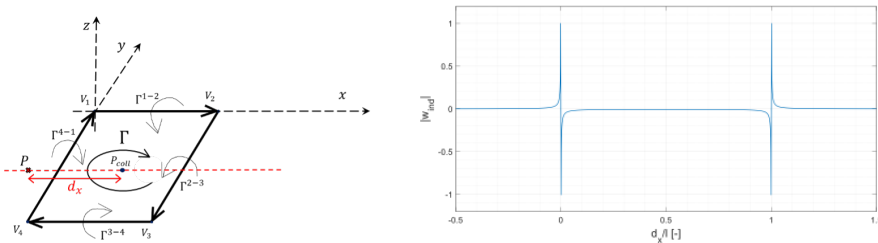


**Figure 3.** Vertical induced velocity (right) by a vortex ring at a collocation point that moves along a longitudinal line (dashed red line in the left picture).

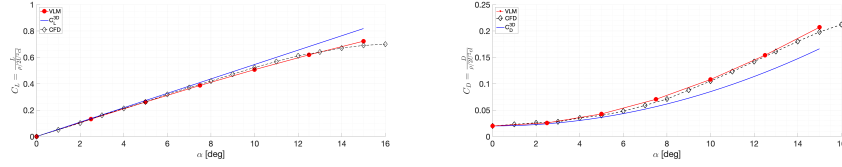


**Figure 4.** Comparison of the  $C_L$  and  $C_D$  for a submerged flat plate,  $AR=3$ .  $Re = 8 \cdot 10^4$ .

$$\mathbf{v}_i = \frac{\Gamma_i}{4\pi} \frac{\mathbf{r}_1 \times \mathbf{r}_2}{|\mathbf{r}_1 \times \mathbf{r}_2|^2} \mathbf{r}_0 \cdot \left( \frac{\mathbf{r}_1}{r_1} - \frac{\mathbf{r}_2}{r_2} \right) \quad (8)$$

Each of the BCs in Eqs. (5) is then written in discrete form by using Eqs. (8) to compute the term related to the derivatives of the potential  $\phi$ , representing the induced velocities. The circulation strengths of the vortex rings of the body and the free surface are the unknown to be found by solving the linear system of equations raising from Eqs. (5). Once the values of  $\Gamma$  are known, the linearized free surface elevation  $\eta$  and the pressure  $p = -\rho g(z + \eta(x, y)) - \rho U \partial \phi / \partial x$  can be computed from the DBC. From the pressures the lift and the induced drag can then be found.

### 3. Sensitivity of the VLM with Respect to the Free Surface Elevation Prediction

The method has been validated by comparison against both experimental measurements and results from other CFD methods (15). For a flat plate,  $AR=3$ , Figure 4 shows the comparison between the predicted  $C_L$  and  $C_D$  by using the proposed VLM, a high-fidelity RANS based CFD method (19) and approximate 2D theoretical formulations corrected for the  $AR$ . The VLM is able to predict the correct values of both coefficients over the lift linear trend. The sensitivity of the free surface prediction with respect to the size of the free surface elements and the ratio  $dh/c$  have been studied. Results of this analysis are shown in Figure 5. The size of the free surface elements is computed as the ratio between their area and the chord of the plate,  $ds/c$ . The effect of this ratio (left picture) is inversely proportional to the accuracy of the predicted free surface elevation. Indeed, a convergence on its shape is found as  $ds/c \rightarrow 0$ . Considering the shifting of the collocation points, convergence is revealed for  $dh/c > 0.1$ , without any significant change above this value. The effect of the depth ratio  $T/c$  has then been analyzed. In particular, four values have been considered, namely  $T/c = [0.3, 1.0, 3.0, 10.0]$ . Figure 6 displays the results of this analysis in terms of lift and drag coefficients and free surface elevation. Compared to the values for deeply submerged plate,  $C_L/C_{L\infty}$  and  $C_D/C_{D\infty}$ , the free surface has a

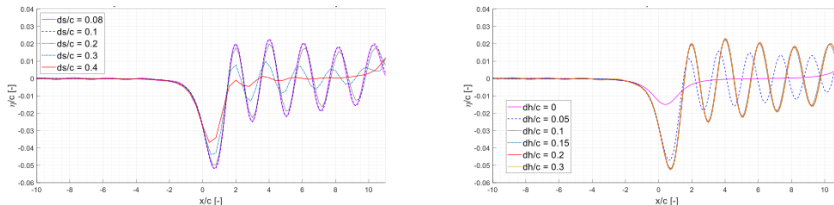


**Figure 5.** Effect of the model parameters: free surface element size  $ds/c$  (left) and collocation point desingularization distance  $dh/c$  (right).  $\alpha = 5^\circ$ .  $Fr = 0.58$ .

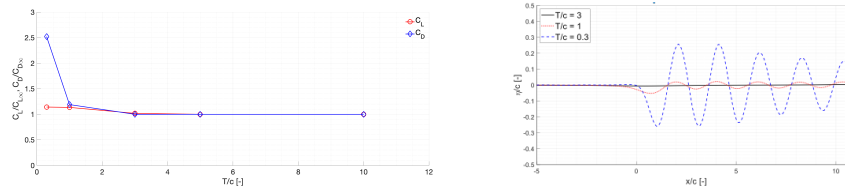


**Figure 6.** Effect of the depth ratio.  $\alpha = 5^\circ$ .  $Fr = 0.58$

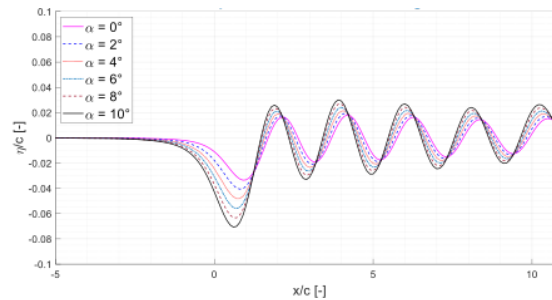


**Figure 7.** Effect of the angle of attack on the free surface elevation at fixed  $T/c = 1.0$ .  $Fr = 0.58$

relevant effect for  $T/c < 3.0$ . The free surface changes consistently in terms of wave height, which increases as  $T/c$  decreases, that is as the body moves closer to the free surface.

The last analysis concerns the variation of the free surface elevation for increasing angles of attack of the plate, in the range  $\alpha = [0^\circ; 10^\circ]$ . As expected, the disturbance to the flow increases with the angle of attack, resulting in higher wave heights. Moreover, the first wave crest and, consistently, all the other peaks and troughs are anticipated as  $\alpha$  increases.

#### 4. Conclusions

A Vortex Lattice Method (VLM) has been developed to study the hydrodynamics performance of lifting bodies moving beneath a free surface. The theoretical framework has been presented, focusing on the linearization of the problem and on the mathematical and numerical treatment of the free surface boundary conditions.

The computational method has been analyzed in terms of sensitivity of the results with respect to some of the model parameters, such as the size of the free surface elements and the distance used for the desingularization of the free surface collocation points. The VLM has also been applied to study the performance of a finite flat plate of  $AR=3$ . In particular, the effect of the depth has been analyzed, showing that for  $T/c > 1.0$  the free surface effect on the lift and drag of the flat plate becomes negligible and, in turn, the flat plate does not affect the free surface elevation anymore. The last analysis has dealt with the effect of the angle of attack, at fixed depth ratio, revealing that, as  $\alpha$  increases, the predicted wave presents higher amplitudes and anticipated positions of the peaks.

## References

- [1] Bal S, Kinnas S. A BEM for the prediction of free surface effects on cavitating hydrofoils. *Computational Mechanics*. 2002;28(3):260-74.
- [2] Faltinsen OM, Semenov YA. The effect of gravity and cavitation on a hydrofoil near the free surface. *Journal of Fluid Mechanics*. 2008;597:371-94.
- [3] Ghassemi H, Kohansal A. Wave generated by the NACA4412 hydrofoil near free surface. 2013.
- [4] Brizzolara S, Young YL. Physical and theoretical modeling of surface-piercing hydrofoils for a high-speed unmanned surface vessel. In: *International Conference on Offshore Mechanics and Arctic Engineering*. vol. 44915. American Society of Mechanical Engineers; 2012. p. 831-7.
- [5] Prasad B, Hino T, Suzuki K. Numerical simulation of free surface flows around shallowly submerged hydrofoil by OpenFOAM. *Ocean Engineering*. 2015;102:87-94.
- [6] Clement E, Hoyt III J. A parametric study of dynaplane-type planing motorboats. In: *First Chesapeake Power Boat Symposium*, Annapolis, MD; 2008. .
- [7] Brizzolara S, Judge C, Beaver B. High deadrise stepped cambered planing hulls with hydrofoils: SCPH2 [C]. In: *A Proof of Concept. SNAME Chesapeake Power Boat Symposium*; 2016. .
- [8] James RM. On the remarkable accuracy of the vortex lattice method. *Computer Methods in Applied Mechanics and Engineering*. 1972;1(1):59-79.
- [9] Konstantinopoulos P, Thrasher D, Mook D, Nayfeh A, Watson L. A vortex-lattice method for general, unsteady aerodynamics. *Journal of aircraft*. 1985;22(1):43-9.
- [10] Young YL, Savander BR. Numerical analysis of large-scale surface-piercing propellers. *Ocean engineering*. 2011;38(13):1368-81.
- [11] Chen Q, Yang CJ, Dong XQ. A Vortex-Lattice Modeling Approach for Free-Surface Effects on Submerged Bodies and Propellers. In: *Practical Design of Ships and Other Floating Structures*. Springer; 2019. p. 636-52.
- [12] Lai C, Troesch AW. Modeling issues related to the hydrodynamics of three-dimensional steady planing. *Journal of Ship research*. 1995;39(01):1-24.
- [13] Migeotte G. Design and optimization of hydrofoil-assisted catamarans. Stellenbosch: Stellenbosch University; 2002.
- [14] Brizzolara S, Vernengo G. A three-dimensional vortex method for the hydrodynamic solution of planing cambered dihedral surfaces. *Engineering Analysis with Boundary Elements*. 2016;63:15-29.
- [15] Solari R, Bagnerini P, Vernengo G. A Vortex Lattice Method for the Hydrodynamic Solution of Lifting Bodies Traveling Close and Across a Free Surface. *WSEAS Transactions on Fluid Mechanics*. 2022;17:39-48.
- [16] Dawson C. A practical computer method for solving ship-wave problems. In: *Proceedings of Second International Conference on Numerical Ship Hydrodynamics*; 1977. p. 30-8.
- [17] Thiart G. Vortex lattice method for a straight hydrofoil near a free surface. *International shipbuilding progress*. 1997;44(437):5-26.
- [18] Katz J, Plotkin A. *Low-speed aerodynamics*. vol. 13. Cambridge university press; 2001.
- [19] Malik K, Asrar W, Sulaeman E. Low Reynolds number numerical simulation of the aerodynamic coefficients of a 3D wing. *International Journal of Aviation, Aeronautics, and Aerospace*. 2018;5(1):8.